THE ASTRONOMICAL JOURNAL, 116:1447–1460, 1998 September

NEAR-INFRARED PHOTOMETRIC STUDIES OF RZ CASSIOPEIAE

WATSON P. VARRICATT, N. M. ASHOK, AND T. CHANDRASEKHAR
Physical Research Laboratory, Navrangpura, Ahamedabad 380009, India; watson@prl.ernet.in, ashok@prl.ernet.in, chandra@prl.ernet.in
Received 1998 April 15; revised 1998 June 1

ABSTRACT

Light curves of the Algol-type binary system, RZ Cassiopeiae, in the near-IR wavelengths J and K are obtained for the first time. The light curves are analyzed using the Wilson-Devinney model. UBV light curves of RZ Cas obtained by Chambliss are also reanalyzed using the same program. In the J and K bands, the bolometric albedo of the secondary of RZ Cas exhibited values above 0.7, whereas the theoretically expected value for such a star is 0.5. Also, the values of the secondary temperature derived from the J and K light curves are found to be less than that derived from our analysis of the optical light curves as well as from the previous studies in the optical photometric bands. We have attempted to model these effects with a dark spot on the secondary of RZ Cas. The J-band light curve gave a better fit with a cool dark spot on the secondary. Another possible reason for the above mentioned effects is a gas stream from the lobe-filling secondary to the primary star. The magnitudes and colors of the individual components are derived from the observed light curves and the light contributions from the stars derived from the light curve analysis. The primary is found to be an A3 V star as observed by previous investigators. The secondary is classified as K0–K4 IV from the derived colors. Seven epochs of primary minima and 3 epochs of secondary minima are obtained from the observations. Because of the increased depths of the secondary eclipse in the infrared bands, the moments of minima are calculated with nearly the same accuracy as that of the primary minima. All the secondary minima are found to occur at phase 0.5. None of the observed primary minima are flat as found by many observers before at optical wavelengths. The colors of the system at the minima obtained by us confirm that the system is partially eclipsing.

Key words: binaries: eclipsing — stars: activity — stars: individual (RZ Cassiopeiae) — stars: spots

1. INTRODUCTION

RZ Cassiopeiae (RZ Cas, HD 17138, HR 815, SAO 12445, BD +69°179) is a semidetached eclipsing binary system of the Algol type. Its variability was discovered by G. Muller in 1906. Being a bright system with very deep primary eclipses in the optical wavelengths ($V = 6.18$ mag, $\Delta V = 1.5$ mag) extensive photometric light curve study of this star has been done by many observers (Huffer 1955; Huffer & Kopal 1951; Chambliss 1976; Riazi, Bagheri, & Faghihi 1994; Maxted, Hill, & Hilditch 1994; Narusawa, Nakamura, & Yamasaki 1994).

This system was found to exhibit disturbances in the light curves especially during the primary eclipse. The period was found to have frequent variations. Photometric analysis by all previous observers show this system to be a partially eclipsing one though many observers have reported primary minima with a flat bottom lasting for several minutes (Szafraniec 1960; Arganbright, Osborn, & Hall 1988; Hegedus 1989; Narusawa et al. 1994). The colors of the system at the primary minima were also found to indicate partial eclipses only. Light curve distortions are observed at the primary minima, often as a rise in flux near the mid-eclipse. Olson (1982) described this as the probable indication of a disklike bulge around the equator of the gainer (primary) and a gas stream from the subgiant secondary to the primary. He also proposed an asymmetric distribution of brightness of the disk owing to the presence of a hot spot where the stream impinges on the disk. The cause of the flat minimum is still not satisfactorily explained.

Hall (1989) observed that the secondaries of Algol binaries are qualified to be included among the class of stars showing chromospheric activity. They satisfy the two main criteria that are believed to be responsible for chromospheric activity: rapid rotation and convection. In Algols, the secondary eclipse is often very shallow in the optical photometric bands since the primary is much brighter than the secondary at optical wavelengths. But in the near-IR wavelengths, the depth of the secondary eclipse increases since the relative contribution of the secondary component to the total system light increases toward longer wavelengths. To resolve the surface features of the secondary, we need to observe the system at wavelengths where the secondary component contributes significantly toward the total observed light and a deeper secondary eclipse will help in determining the surface features of the secondary, especially on its inner hemisphere. Also, free-free emission from a gas stream or circumstellar plasma will contribute significantly in the infrared wavelengths. The only existing IR light curves of Algol systems are the 1.2 μm light curve of β Per (Chen & Reuning 1966) and JHK-band light curves of UX Her (Lazaro et al. 1997). Analysis of the IR light curves of β Per by Richards (1990) has revealed time-dependent changes in the depths and phases of both eclipses, asymmetry in the secondary minima and cyclic variations in the mean temperature of the secondary component. The overall variability found was similar to that seen in the optical light curves of RS CVn systems where star spots are believed to play a major role (McCluskey 1993).

Most of the information available about RZ Cas is derived from photometric and a few spectroscopic investigations at optical wavelengths. Observations at radio (Drake, Simon, & Linskey 1986; Umana, Catalano, & Rodono 1991) and X-ray wavelengths (McCluskey &

Kondo 1984; Singh, Drake, & White 1995) gave strong indications of chromospheric and coronal activity in this system. Singh, Drake & White observed soft X-ray spectra from the corona of the active secondary. They also observed variations in the observed X-ray emission, which was attributed to the rotational modulation of compact active regions on the secondary surface or flaring incidents. Observations by Schmitt et al. (1990) also gave indications of a hot corona in RZ Cas, and they calculated the coronal temperature to be $\sim 10^7$ K.

In RZ Cas, the depth of secondary eclipse in the optical photometric bands ($\Delta V = 0.08$ mag) is insufficient to get a clear picture of the features of the secondary star. We have attempted to study the light curves of this system in the near infrared bands, J and K, in which the secondary minima are much deeper compared to those in the optical bands. These are the first observations of this binary in the near infrared bands.

2. OBSERVATIONS

Observations were made with the 1.2 m Mount Abu IR Telescope, India, and a near-IR photometer with an LN2 cooled InSb detector during the period from 1995 October 6 to 1996 November 28. The details of the instrument are given in Ashok et al. (1994) and Sam Ragland (1996). The system was observed in the J band for 20 days and in the K band for 15 days. HR 791 and ψ Cas were used as comparison and check stars, respectively. HR 791, though a spectroscopic binary star, was used as a comparison star for the optical observations of RZ Cas by several observers owing to its similarity in spectral type and brightness to RZ Cas (Huffer 1955; Chambliss 1976; Argenbright et al. 1988). Also, in the J and K bands this star is bright enough for our system to get a good signal to noise ratio with the same integration time as used for RZ Cas.

There are no previous infrared observations existing for HR 791 to the best of our knowledge. The observed J-, H-, and K-band magnitudes and colors of HR 791 and ψ Cas are given in Table 1. The $J-H$ and $H-K$ colors of HR 791 observed by us are typical for a star of spectral type A5 III as determined from optical observations. ψ Cas was observed by Neugebauer & Leighton (1969) in the 2 μm Sky Survey. $J-H$ and $H-K$ colors of this star correspond to a star of spectral type K0 III as found by previous investigators. The observed J and K magnitudes of RZ Cas at phase 0.25 and eclipse depths (with respect to the magnitude at phase 0.25) are given in Table 2. The primary standard used for photometry was HR 696 (Elias et al. 1982; Scott 1988). BD $+57°647$ (Scott 1988) was also observed. Each observation was done with an integration time of 20 s. Typical errors of observations are ± 0.03 mag in J band and ± 0.04 mag in the K band.

The observations of RZ Cas and HR 791 were done in the sequence C-V-V-C with observations of ψ Cas two to three times per night. V refers to the variable star under study and C, the comparison star. The first order extinction coefficient for each night was obtained by doing a linear least square fit to the observed instrumental magnitudes of the comparison star and an extinction correction is applied to the observed relative magnitudes of RZ Cas. We have not applied color corrections as observations were always done in a single band. A total of 839 and 947 individual observations of RZ Cas were obtained in the J and K band, respectively, with good coverage of phase. The epochs of observations, phases, and the observed relative magnitudes are given in Tables A1 and A2, respectively. Figure 1 shows the observed points in the J band. Figure 2 shows the observed light curve of RZ Cas in the K band along with the $J-K$ color curve.

Seven epochs of primary minima (five in J band and two in K band) and 3 epochs of secondary minima (one in J band and two in K band) are observed. Epochs of minima are calculated using the method given by Kwee & van Woerden (1956). The epochs of secondary minima are determined with similar accuracies to that of the epochs of primary minima due to the enhanced depths of the secondary eclipses in the J and K bands compared to those in the optical bands. The epochs determined, errors, bands of observations, number of points and type of minima (primary, PM, or secondary, SM) are given in Table 3. None of the minima show a flat bottom. We have derived a new ephemeris for RZ Cas by doing a linear least squares fit to our observed epochs of primary minima:

$$\text{JD Hel. Min } I = 2{,}450{,}020.4070(\pm 0.0005) + 1.1952592(\pm 0.000004)E_0 \text{ days} . \quad (1)$$

The phases for constructing our J and K light curves are calculated according to this new ephemeris. All secondary

TABLE 1

OBSERVED JHK MAGNITUDES AND COLORS OF HR 791 AND ψ CASSIOPEIAE

Star Name	J	H	K	$V-K$	$J-H$	$H-K$
HR 791.....	5.71	5.67	5.63	0.32	0.04	0.04
ψ Cas.....	3.01	2.48	2.41	2.33	0.53	0.07

TABLE 2

OBSERVED MAGNITUDES AND ECLIPSE DEPTHS OF RZ CASSIOPEIAE IN THE J AND K BANDS

Photometric Band	Magnitude at Maximum Brightness	Eclipse Depth	
		Primary	Secondary
J.....	5.76	1.08	0.21
K.....	5.50	0.87	0.30

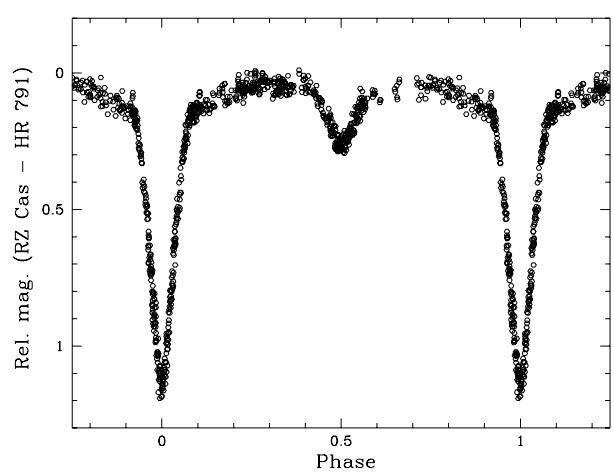

FIG. 1.—Observed points (relative magnitude RZ Cas-HR 791) in the J band.

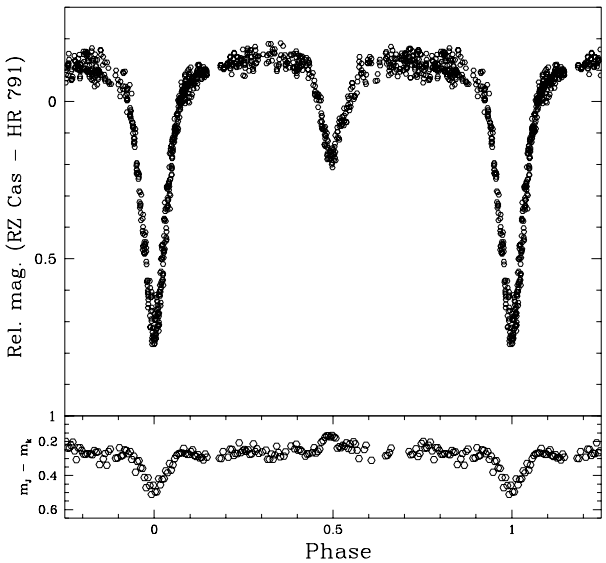

FIG. 2.—(*Top*) Observed points (relative magnitude RZ CasS-HR 791) in the K band. (*Bottom*) $J-K$ color curve binned in phase intervals of 0.005.

minima appeared at phase 0.5 and the primary and the secondary eclipses were observed to be of equal widths implying a circular orbit.

3. LIGHT CURVE ANALYSIS

The Wilson-Devinney model (Wilson & Devinney 1971; Wilson 1979, 1993) is used to analyze the light curves of RZ Cas. The J and K light curves observed in the present program are analyzed, and the results are compared with the results of our analysis of the UBV light curves (obtained by Chambliss 1976) done as a part of the present study.

3.1. *Analysis of the J and K-Band Light Curves*

The observed relative magnitudes are converted to light units. The average relative magnitude (RZ Cas-HR 791) at phase 0.25 in each band is subtracted from the observed light curve in the corresponding band and the resulting relative magnitude values are converted into relative light values. The light curves are then averaged in phase intervals of 0.01 phases. 92 and 95 normal points are formed in J and K bands, respectively. Each data point is weighted with the number of individual points averaged to form the normal point.

Wilson's program needs a set of parameters reasonably near the solution to start with. We have adopted the values given by Chambliss (1976) as a starting set of parameters for the analysis of J-band data. The output values of the J-band analysis are used as starting values for the analysis of the K-band data. Mode 5 (for the semidetached systems) is selected and differential corrections are applied to the light curves. The program parameter noise = 2 is selected so that observational scatter is assumed to depend upon light levels. Both the light curves are analyzed separately as well as simultaneously. The mass ratio, q, for RZ Cas is determined by Maxted et al. (1994) with good accuracy from the radial velocity curves of both the primary and the secondary. The value of q obtained by them (0.33107) is close to those used by previous observers [Chambliss 1976 (0.35); Duerbeck & Hanel 1979 (0.35); Narusawa et al. 1994 (0.319)]. So we have adopted q as determined by Maxted et al. as a fixed parameter in the light curve fitting. F_2, the ratio of the axial rotation to the mean orbital rotation for the secondary star was adopted to be 1. Since the secondary is a lobe-filling component in this close binary system, it is justifiable to consider it to be a synchronous rotator. The corresponding parameter, F_1, for the primary, though left as a free parameter in the initial iterations with 1.000 as the starting value, did not vary by more than its probable error. So the value of F_1, was fixed to be 1.000 in further iterations. The gravity darkening coefficients, g_1 and g_2, were fixed to their theoretical values of 1.00 and 0.32, respectively for the primary and the secondary (Von Zeipel 1924; Lucy 1967).

The primary is known to be an A3 V star from previous photometric and spectroscopic studies (Maxted et al. 1994). So we have fixed the average effective temperature of the primary, T_1, to be 8720 K, corresponding to an A3 V star (Lang 1992) in the analysis. The secondary temperature, T_2, is left as a free parameter throughout the analysis. Small changes in the value of limb darkening are found to have only a mild effect on the light curve. So the values of the limb darkening were fixed to their theoretical values. A linear law was adopted to represent the limb darkening effect. Wavelength specific limb darkening coefficients were taken from Al Naimiy (1978) and bolometric limb darkening coefficients for the treatment of the reflection effect were taken from Van Hamme (1993). The number of reflections, NREF, was taken as 1 during the initial iterations and was changed to 2 during the final iterations. Increasing the number of reflections from 1 to 2 had only a minor effect on the corrections to the parameters. The control integer in the model IPB is selected to be 0 so that the luminosity of the secondary, L_2, is calculated from the temperatures, T_1 and T_2, luminosity of the primary star, L_1, system geometry, and the radiation laws. L_1 is left as a free parameter. Model atmosphere corrections are applied to the primary star luminosity. For calculating L_2, the secondary is considered as a blackbody since its temperature is below 5000 K and the atmospheric model used by Wilson's program (Carbon & Gingerich 1969) is recommended for atmospheres only above 5000 K. We have tried to look for the possibility of the presence of a third component in the system, letting l_3 be free during the initial iterations. The analysis did not give any signature of third light. Corrections for l_3 fluctuated around the starting value 0.000. So after a few iterations l_3 was fixed to 0.000. In mode 5 for Algol-type systems, the potential representing the secondary surface, Ω_2, is determined within the program from the lobe-filling condition for the given mass ratio. The corresponding potential for

TABLE 3

OBSERVED EPOCHS OF MINIMA OF RZ CASSIOPEIAE

Epoch of Minimum (HJD)	Band	Number of Points	Minima Type
2,450,017.4178 ± 0.0007.....	K	69	SM
2,450,032.3587 ± 0.0008.....	K	71	PM
2,450,035.347 ± 0.001	J	35	SM
2,450,037.1411 ± 0.0005.....	J	35	PM
2,450,062.2402 ± 0.0005.....	J	49	PM
2,450,092.1244 ± 0.0004.....	J	33	PM
2,450,093.3174 ± 0.0003.....	J	37	PM
2,450,114.2288 ± 0.0005.....	K	27	SM
2,450,117.2228 ± 0.0005.....	J	50	PM
2,450,387.3514 ± 0.0004.....	K	27	PM

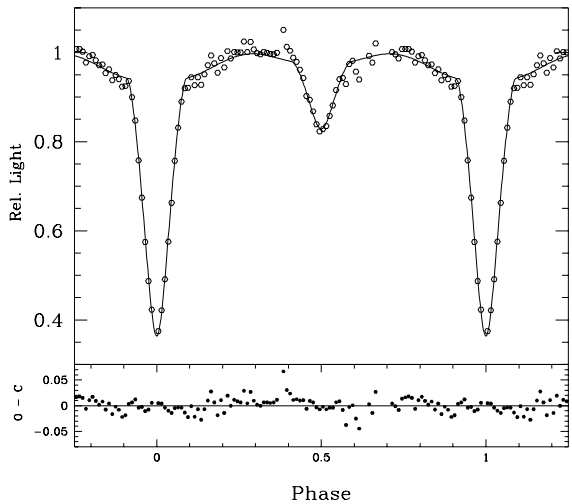

FIG. 3.—J-band light curve of RZ Cas and the residuals. The hexagons in the top panel show the normal points formed from the observed light curve, and the solid line shows the model fit with $A_2 = 0.5$. The bottom panel shows the deviations of the observed points from the model.

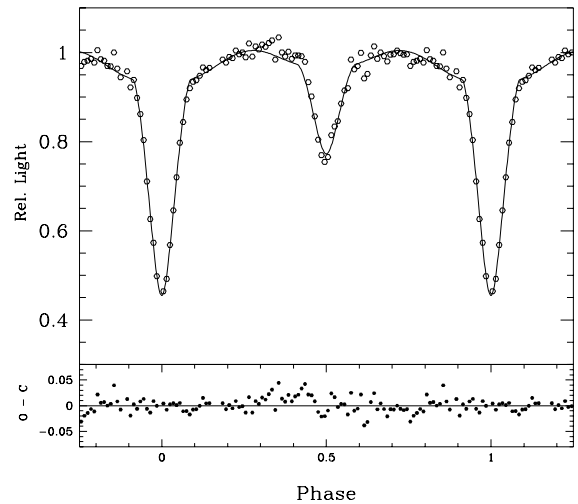

FIG. 4.—K-band light curve of RZ Cas and the residuals. The hexagons in the top panel show the normal points formed from the observed light curve, and the solid line shows the model fit with $A_2 = 0.5$. The bottom panel shows the deviations of the observed points from the model.

the primary surface, Ω_1, is taken as a free parameter during the analysis. The bolometric albedos of the atmospheres of the primary and secondary stars, A_1 and A_2, which parameterize the reflection effect, were fixed to their theoretical values of 1.0 and 0.5 (Rucinski 1969), respectively.

Table 4 shows the results of the light curve fits in J and K bands with the complete set of parameters. (In the tables, a superscript f implies that the corresponding parameter was fixed during the analysis.) Figures 3 and 4 show the model fits in the J and K bands, respectively, along with the normal points formed for the analysis and the residuals of the fit. The fit is poor outside of the primary minimum, where residuals are found systematically positive or negative in different regions of the light curve. The light curves are divided into eight sectors based on the phases of minima and eclipse duration (0.17 × Period) and the residuals for all sectors are calculated. The arithmetic mean and the rms values of the residuals (observed − model) in the different sectors of the light curve are given in Table 7. This table brings out clearly the poor fit and the asymmetry in the light curve, especially in the regions before and after the secondary minimum (the model that we have adopted is symmetric). The large positive residuals near the ingress and

TABLE 4

ELEMENTS OBTAINED FROM THE ANALYSIS OF J AND K-BAND DATA WITH $A_2 = 0.5$

			J AND K COMBINED	
PARAMETER	J	K	J	K
T_1^f (K)	8720	8720	8720	
T_2 (K)	4163 ± 30	4249 ± 36	24190 ± 25	
q^f	0.33107	0.33107	0.33107	
i (deg)	82.548 ± 0.111	81.806 ± 0.113	82.247 ± 0.079	
Ω_1	4.2358 ± 0.0510	4.3835 ± 0.0497	4.3288 ± 0.0516	
Ω_2	2.5339	2.5339	2.5339	
$r_{1\mathrm{pole}}$	0.2554 ± 0.0033	0.2461 ± 0.0030	0.2495 ± 0.0020	
$r_{1\mathrm{point}}$	0.2612 ± 0.0036	0.2510 ± 0.0033	0.2547 ± 0.0021	
$r_{1\mathrm{side}}$	0.2583 ± 0.0035	0.2486 ± 0.0031	0.2522 ± 0.0020	
$r_{1\mathrm{back}}$	0.2603 ± 0.0036	0.2503 ± 0.0033	0.2540 ± 0.0021	
$r_{2\mathrm{pole}}$	0.2684	0.2684	0.2684	
$r_{2\mathrm{point}}$	0.3886	0.3886	0.3886	
$r_{2\mathrm{side}}$	0.2796	0.2796	0.2796	
$r_{2\mathrm{back}}$	0.3123	0.3123	0.3123	
x_1^f	0.250	0.150	0.250	0.150
x_2^f	0.470	0.320	0.470	0.320
$x_{1\mathrm{bol}}^f$	0.573	0.573	0.573	
$x_{2\mathrm{bol}}^f$	0.528	0.528	0.528	
g_1^f	1.00	1.00	1.00	
g_2^f	0.32	0.32	0.32	
A_1^f	1.000	1.000	1.000	
A_2^f	0.500	0.500	0.500	
$L_1/(L_1 + L_2)$	0.8042 ± 0.0056	0.6796 ± 0.0060	0.7934 ± 0.0039	0.6916 ± 0.0045
$L_2/(L_1 + L_2)$	0.1958 ± 0.0110	0.3204 ± 0.0164	0.2066 ± 0.0081	0.3084 ± 0.0108
l_3^f	0.0000	0.0000	0.0000	0.0000

NOTE.—f is a fixed parameter.

the negative residuals near the egress of the secondary eclipse are noticeable in the arithmetic mean of residuals of both the light curves. The effect is more pronounced in the J band than in the K band. The average value of T_2 derived is 4190 K, which is less than the T_2 derived by Maxted et al. (1994) and Narusawa et al. (1994). It is less by $\sim$300 K than the value of T_2 derived by our own analysis of Chambliss' optical light curves (§ 3.2). The T_2 derived by Chambliss is above 5000 K, much higher than our value, but the model used by him is different and he has adopted 9700 K for T_1, which is higher than the value used by us for T_1 (8720 K).

We have attempted to fit the light curves with Ω_2 as a free parameter, adopting mode 2 of the program, looking for the possibility of a detached configuration. But most of the time Ω_2 went below the critical value, which is an unphysical situation according to the adopted model where the secondary star becomes bigger than its Roché lobe. So as in the case of all of the previous investigations, this study also reveals that the system is in the semidetatched state.

3.1.1. *Models With A_2 as a Free Parameter*

For a binary system of the Algol type, where the primary star is hotter than the secondary, often by a factor of 2 or more, the heating of the facing hemisphere of the primary, by the secondary star is negligible, whereas the heating of the facing hemisphere of the secondary star by the hotter primary star is considerable and it will have significant effect on the observed light curve (Wilson 1990). Since the nature of the observed light curves outside the eclipses resembled the presence of a high bolometric Albedo for the secondary star, light curve fitting was again done with A_2 as a free parameter. A_1 was fixed to its theoretical value 1.00. In both J and K light curve analyses and in the combined analysis, A_2 when taken to be a free parameter, converged to a value greater than 0.7. The complete set of fitted parameters is given in Table 5. The problem of finding high A_2 in the light curves of Algol secondaries was faced in the light curve analysis of many Algols by different investigators. Van Hamme & Wilson (1993) obtained values of $A_2 \sim 0.7$ and $A_2 \sim 0.8$ for S Cnc and TT Hya, respectively. They have called for a revised treatment of reflection from convective atmospheres. In the case of RZ Cas, Maxted et al. (1994) obtained a high A_2 in the analysis of the U and B light curves.

The value of T_2 derived from the analysis of J and K light curves is less than that derived from the light curves in UBV bands by 250 K. This is more than indicated by the error limits. The situation of T_2 being lower in the near-IR bands compared to that in the optical did not improve much with A_2 as free parameter. This problem of finding different values of T_2 at different wavelengths is observed frequently in the analysis of the light curves of many Algols (Chambliss 1976; Van Hamme & Wilson 1986, 1990, 1993). In Wilson's program, the control parameter IPB can be selected as 1 to determine L_2 independently of T_2, so that we can assign the same value of T_2 to all the light curves and adjust L_2 as a free parameter. We have not adopted this method in the present study; instead, we looked for alternate methods to solve it, which will be explained in the next subsection.

The orbital inclination derived from the J and K light curves is less than that derived from the UBV light curves by $\sim 1°$. The fitted light curves are shown in Figures 5 and 6. The model light curves shown are generated with the parameters obtained in the J and K individual analysis. We can see that the fit has improved slightly with a high value of A_2. But still systematic residuals are present in the region outside eclipse and we end up with some new problems.

The secondary is a subgiant star of mass 0.73 $M_\odot$, and theoretically it is expected to have a convective atmosphere. The bolometric albedo of such an atmosphere should be 0.5

TABLE 5

ELEMENTS OBTAINED FROM THE ANALYSIS OF J AND K-BAND DATA WITH A_2 AS A FREE PARAMETER

			J AND K COMBINED	
PARAMETER	J	K	J	K
T_1^f (K)	8720	8720	8720	
T_2 (K)	4204 ± 32	4317 ± 38	4257 ± 26	
q^f	0.33107	0.33107	0.33107	
i (deg)	82.482 ± 0.106	81.839 ± 0.107	82.210 ± 0.071	
Ω_1	4.2795 ± 0.0403	4.4041 ± 0.0660	4.3700 ± 0.0436	
Ω_2	2.5339	2.5339	2.5339	
$r_{1\,\mathrm{pole}}$	0.2526 ± 0.0026	0.2449 ± 0.0039	0.2470 ± 0.0003	
$r_{1\,\mathrm{point}}$	0.2581 ± 0.0028	0.2498 ± 0.0043	0.2520 ± 0.0003	
$r_{1\,\mathrm{side}}$	0.2554 ± 0.0027	0.2474 ± 0.0041	0.2495 ± 0.0003	
$r_{1\,\mathrm{back}}$	0.2573 ± 0.0028	0.2490 ± 0.0042	0.2512 ± 0.0003	
$r_{2\,\mathrm{pole}}$	0.2684	0.2684	0.2684	
$r_{2\,\mathrm{point}}$	0.3886	0.3886	0.3886	
$r_{2\,\mathrm{side}}$	0.2796	0.2796	0.2796	
$r_{2\,\mathrm{back}}$	0.3123	0.3123	0.3123	
x_1^f	0.250	0.150	0.250	0.150
x_2^f	0.470	0.320	0.470	0.320
$x_{1\,\mathrm{bol}}^f$	0.573	0.573	0.573	
$x_{2\,\mathrm{bol}}^f$	0.528	0.528	0.528	
g_1^f	1.00	1.00	1.00	
g_2^f	0.32	0.32	0.32	
A_1^f	1.000	1.000	1.000	
A_2	0.720 ± 0.058	0.744 ± 0.069	0.731 ± 0.044	
$L_1/(L_1 + L_2)$	0.7959 ± 0.0054	0.6706 ± 0.0087	0.7821 ± 0.0037	0.6804 ± 0.0027
$L_2/(L_1 + L_2)$	0.2041 ± 0.0080	0.3294 ± 0.0215	0.2179 ± 0.0106	0.3196 ± 0.0123
l_3^f	0.0000	0.0000	0.0000	0.0000

NOTE.—f is a fixed parameter.

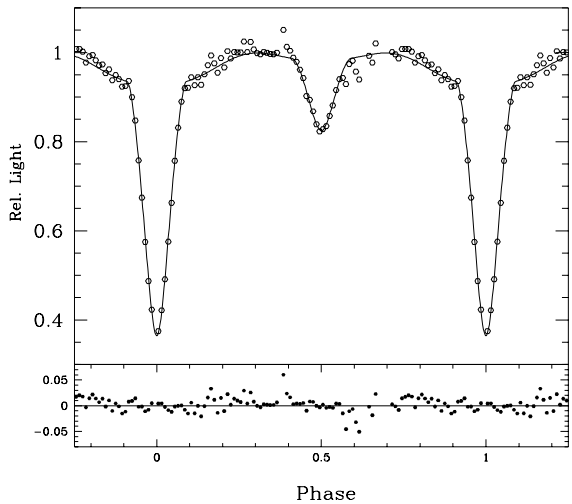

FIG. 5.—J-band light curve of RZ Cas. The hexagons in the top panel show the normal points formed from the observed light curve, and the solid line shows the model fit with A_2 as a free parameter. The bottom panel shows the deviations of the observed points from the model.

(Rucinski 1969). In our reanalysis of the UBV light curves of Chambliss (1976) (see § 3.2), A_2, when considered as a free parameter, oscillated around the value 0.5 and the program gave a good fit to the observed light curves for $A_2 = 0.5$. In all the existing models of binary star light curve analysis, the reflection effect is treated bolometrically and the parameter A_2 is wavelength independent. So it is puzzling to see how the light curves of a star in different wavelengths can have different bolometric albedos. This will lead us to the following conjectures:

1. If the higher A_2 (compared to the theoretical value and what we derived from the optical observations) that we find in the J and K bands is real, then we have to reconsider the treatment of reflection in the existing models, i.e., whether we should think about a wavelength-dependent reflection effect viz., absorption in certain wavelengths and reemission in certain other wavelengths locally.

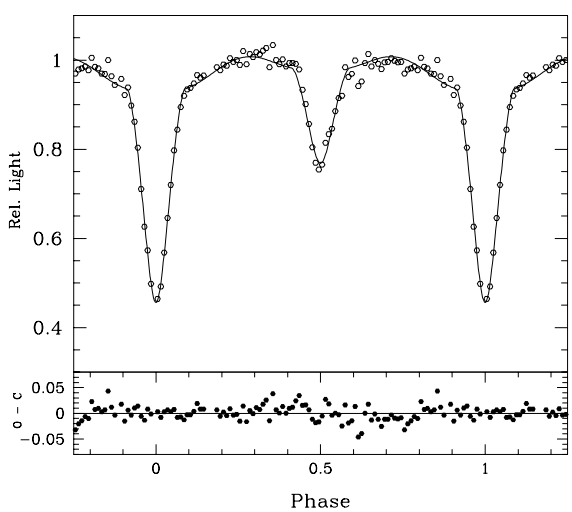

FIG. 6.—K-band light curve of RZ Cas. The hexagons in the top panel show the normal points formed from the observed light curve, and the solid line shows the model fit with A_2 as a free parameter. The bottom panel shows the deviations of the observed points from the model.

2. Is our concept about the atmosphere of the secondary star, being convective, correct? Since we find a higher albedo A_2 in the J and K bands, is it possible that it is not totally convective? Or should we think that A_2 may not be 0.5 for a convective atmosphere?[1] Then why do we see an albedo of 0.5 in the UBV light curves (taken only two decades before the present study), which agrees very well with the theoretical value for a convective atmosphere? So the discrepancy in the value of A_2 that we see is unlikely to be an indication of a departure of the photosphere from convective nature.

3. Does the high A_2 that we obtained from the analysis of the J and K light curves result from any other parameter not properly taken care of in the analysis or in the model? One possibility is the presence of a cool spot on the back side (longitude = 180°) of the secondary star. This can reproduce the slope seen outside the minima similar to that produced by a high A_2. So an attempt is made to model the light curves with a single spot on the back of the secondary star and the results are presented in § 3.1.2.

4. The presence of a gas stream in the system, oriented toward the pole of the primary due to the bipolar magnetic field of the primary also can mimic a high A_2, since we may see parts of the primary through the stream before and after the primary eclipse. This can also reproduce the asymmetry of the light curve, seen as a maculation at around phase 0.6, due to absorption of the light from the secondary star by the stream, which is deviated from a radial path due to the Coriolis force. The modeling of a stream is not attempted in this paper.

3.1.2. *Model With a Single Spot on the Secondary Star*

In the previous section we have indicated the possibility of explaining the distortions in the light curve outside the minima by invoking a cool spot on the secondary star. Accordingly, a dark spot was adopted on the secondary star. To begin with, the spot parameters were selected by trial and error. The iteration was started with a suitable set of numbers for the spot parameters. The spot parameters were kept fixed and the iterations were done for the set of system parameters i, T_2, A_2, Ω_1, and L_1. It was noticed that A_2 came down to a value near 0.5. The secondary temperature T_2 also increased by more than 100 K in both J and K. Thus, the situation of the discrepancy of T_2 being smaller in the present analysis of the J and K light curves was reduced with the inclusion of a cool spot on the secondary star.[2] After attaining convergence in the system parameters, we released the spot parameters free and tried fitting for the spot. Though convergence was obtained for each spot parameter separately, the error estimates of the spot parameters were too high when all the spot parameters were considered free simultaneously. So the spot parameters were fixed to the converged values and system parameters were again determined. The derived system parameters are given along with the adopted spot parameters in Table 6. The fitted light curves and residuals in the J and K bands are given in Figures 7 and 8, respectively, and the arithmetic

[1] This question was previously raised by Van Hamme & Wilson (1993).

[2] This is obviously expected since we are fixing the temperature of the primary and darkening some portion of the secondary star. So to keep the luminosity of the model fit in agreement with the observed total luminosity, the temperature of the secondary will increase.

TABLE 6

ELEMENTS OBTAINED FROM THE ANALYSIS OF J AND K-BAND DATA WITH A COOL SPOT ON THE SECONDARY STAR

			J AND K COMBINED	
PARAMETER	J	K	J	K
T_1^f (K)	8720	8720	8720	
T_2 (K)	4349 ± 30	4415 ± 44	4359 ± 28	
q^f	0.33107	0.33107	0.33107	
i (deg)	82.099 ± 0.086	81.542 ± 0.111	82.013 ± 0.076	
Ω_1	4.4125 ± 0.0472	4.4010 ± 0.0534	4.4084 ± 0.0448	
Ω_2	2.5339	2.5339	2.5339	
$r_{1\mathrm{pole}}$	0.2444 ± 0.0028	0.2451 ± 0.0032	0.2447 ± 0.0015	
$r_{1\mathrm{point}}$	0.2492 ± 0.0030	0.2500 ± 0.0035	0.2495 ± 0.0016	
$r_{1\mathrm{side}}$	0.2469 ± 0.0029	0.2476 ± 0.0033	0.2471 ± 0.0015	
$r_{1\mathrm{back}}$	0.2485 ± 0.0030	0.2492 ± 0.0034	0.2488 ± 0.0016	
$r_{2\mathrm{pole}}$	0.2684	0.2684	0.2684	
$r_{2\mathrm{point}}$	0.3886	0.3886	0.3886	
$r_{2\mathrm{side}}$	0.2796	0.2796	0.2796	
$r_{2\mathrm{back}}$	0.3123	0.3123	0.3123	
x_1^f	0.250	0.150	0.250	0.150
x_2^f	0.470	0.320	0.470	0.320
$x_{1\mathrm{bol}}^f$	0.573	0.573	0.573	
$x_{2\mathrm{bol}}^f$	0.528	0.528	0.528	
g_1^f	1.00	1.00	1.00	
g_2^f	0.32	0.32	0.32	
A_1^f	1.000	1.000	1.000	
A_2	0.561 ± 0.047	0.491 ± 0.063	0.533 ± 0.038	
$L_1/(L_1+L_2)$	0.7677 ± 0.0062	0.6613 ± 0.0080	0.7669 ± 0.0040	0.6660 ± 0.0042
$L_2/(L_1+L_2)$	0.2323 ± 0.0119	0.3387 ± 0.0201	0.2331 ± 0.0080	0.3340 ± 0.0101
l_3^f	0.0000	0.0000	0.0000	0.0000
Phase Shift	0.0000 ± 0.0001	0.9999 ± 0.0002	0.0000 ± 0.0001	
Spot Parameters:				
Latitude^f	80.00	80.00	80.00	
Longitude^f	175.41	182.64	174.72	
Ang. Rad.^{f}	20.43	20.48	20.53	
Temp. f.^{f}	0.739	0.783	0.743	

NOTE.—f is a fixed parameter.

mean and rms values of the residuals are given in Table 7. The model with a spot better represents the observed light curves, especially in the J band. Since the spot is assumed to be present on the less luminous secondary star, its effect will go unnoticed in the UBV bands. Since the convergence of the spot parameters was not satisfactory at this stage, we would like to propose the spot model only as one of the strong possibilities to explain the discrepancies that we noticed between the analysis of the JK and UBV light curves and as a partial explanation of some of the distortions seen in the J and K light curves. The large-scale activ-

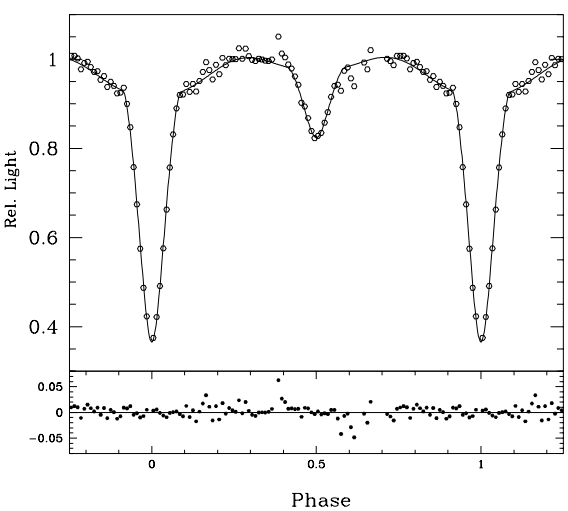

FIG. 7.—J-band light curve of RZ Cas. The hexagons in the top panel show the normal points formed from the observed light curve, and the solid line shows the model fit with one cool spot at the back side of the secondary star. The bottom panel shows the deviations of the observed points from the model.

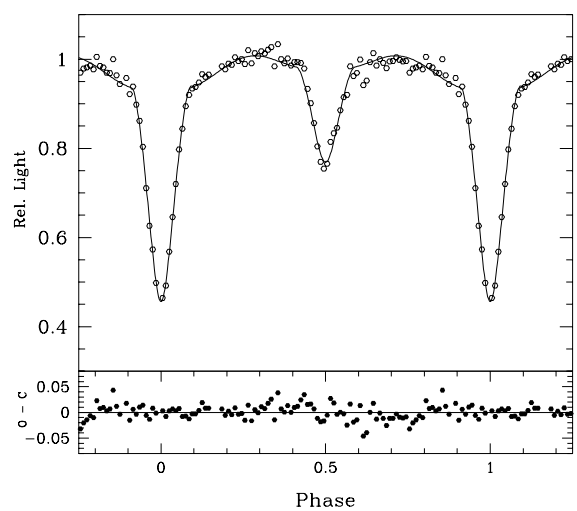

FIG. 8.—K-band light curve of RZ Cas. The hexagons in the top panel show the normal points formed from the observed light curve, and the solid line shows the model fit with one cool spot at the back side of the secondary. The bottom panel shows the deviations of the observed points from the model.

TABLE 7

ELEMENTS OBTAINED FROM THE ANALYSIS OF U, B, AND V LIGHT CURVES OF CHAMBLISS (1976)

				U, B, AND V COMBINED		
PARAMETER	U	B	V	U	B	V
T_1^f (K)	8720	8720	8720		8720	
T_2 (K)	4665(64)	4712(62)	4525(40)		4507(22)	
q^f	0.33107	0.33107	0.33107		0.33107	
i (deg)	83.361(97)	83.306(74)	83.244(75)		83.203(32)	
Ω_1	4.3782(192)	4.3614(97)	4.3700(132)		4.3615(46)	
Ω_2	2.5339	2.5339	2.5339		2.5339	
$r_{1\mathrm{pole}}$	0.2465(11)	0.2475(2)	0.2470(8)		0.2475(1)	
$r_{1\mathrm{point}}$	0.2515(13)	0.2526(2)	0.2520(9)		0.2525(1)	
$r_{1\mathrm{side}}$	0.2490(12)	0.2501(2)	0.2496(8)		0.2501(1)	
$r_{1\mathrm{back}}$	0.2507(12)	0.2518(2)	0.2513(9)		0.2518(1)	
$r_{2\mathrm{pole}}$	0.2683	0.2683	0.2683		0.2683	
$r_{2\mathrm{point}}$	0.3886	0.3886	0.3886		0.3886	
$r_{2\mathrm{side}}$	0.2795	0.2795	0.2795	0.2795		
$r_{2\mathrm{back}}$	0.3123	0.3123	0.3123		0.3123	
x_1^f	0.515	0.554	0.475	0.515	0.554	0.475
x_2^f	0.900	0.800	0.700	0.900	0.800	0.700
$x_{1\mathrm{bol}}^f$	0.573	0.573	0.573		0.573	
$x_{2\mathrm{bol}}^f$	0.537	0.537	0.537		0.537	
g_1^f	1.00	1.00	1.00		1.00	
g_2^f	0.32	0.32	0.32		0.32	
A_1^f	1.000	1.000	1.00		1.000	
A_2	0.500	0.500	0.500		0.500	
$L_1/(L_1 + L_2)$	0.9597(45)	0.9573(35)	0.9306(31)	0.9702(13)	0.9684(12)	0.9324(20)
$L_2/(L_1 + L_2)$	0.0403(57)	0.0427(44)	0.0694(44)	0.0298(15)	0.0316(12)	0.0676(22)
l_3^f	0.0000	0.0000	0.0000	0.0000	0.0000	0.0000

NOTE.—f is a fixed parameter.

ity of the system in the radio and X-ray wavelengths due to chromospheric and coronal activities and the very fact that the secondary star is a late-type fast rotator with a convective envelope encourage us to put more faith in the presence of a cool spot on the secondary star. It is encouraging to note that Maxted et al. (1994) raised the possibility of a dark spot on the secondary to explain the difference in light levels at quadratures seen in the UBV light curves of Chambliss (1976). Umana, Catalano & Rodono (1991) observed RZ Cas with the VLA at 6 cm and derived a brightness temperature of 4.26×10^8 K and 11.1×10^8 K from two observations. Assuming the radio emission to be arising from the gyrosynchrotron radiation from mildly relativistic electrons interacting with the magnetic field of the active component, they derived the mean magnetic field to be 15–150 G for a set of seven Algols. Umana et al. (1993) obtained radio continuum spectra of RZ Cas along with five other Algols at VLA frequencies 1.49, 5, 8.4, and 14.9 GHz. The observed spectra were similar to that of the RS CVns. RZ Cas was detected at X-ray wavelengths also. Schmitt et al. (1990) observed soft X-ray emission from RZ Cas. Singh, Drake & White (1995) observed X-ray emission from RZ Cas along with four other Algols. The emission is interpreted as of coronal origin. RZ Cas showed variable levels of X-ray emission. All these observations give strong indication of the chromospheric activity of the secondary of RZ Cas. More observations of the light curves in the near-IR bands with better accuracy will help us to confirm the presence of spot and to observe any possible migrations.

We have already shown through Table 8 that there is a decrease in the observed light when the system comes out of the secondary eclipse. This maculation type of phenomenon is seen more prominently in the J band and is weak in the K-band light curve. The depression of light in the J band can be fitted well with a spot on the inner surface of the secondary at a longitude greater than 315°. But before proceeding further, let us have a closer look at this maculation type of phenomena. Arévalo & Lázaro (1990) in their J and K light curves of the short-period RS CVn system XY UMa observed an asymmetric secondary minimum with the intensity lower in the ascending branch of the secondary eclipse where it emerges out of the eclipse. They commented that this may be the effect of absorption by a gas stream from the secondary directed toward the pole of the primary. Budding & Zeilik (1987) have noticed maculation minima at phases 0.27 and 0.56 in the V-band light curve of XY UMa and have modeled it with two spots on the secondary. They have analyzed the light curves of 10 short-period RS CVn systems and found maculation minima between phases 0.56 and 0.65 in five systems [XY UMa (0.56), SV Cam (0.60), CG Cyg (0.61), ER Vul (0.65) and UV Psc (0.61)]. A closer look at the 1.2 μm light curve of β Per by Chen & Reuning (1966) and the model fit by Richards, Mochnacki, & Bolton (1988) reveals that there is a mild rise in flux around the beginning of the secondary eclipse and most of the observed values fall below the model curve when the system emerges out of the secondary eclipse. The same 1.2 μm light curve of Chen & Reuning (1966) is analyzed by Wilson et al. (1972) along with UBV light curves observed by them. The normal points formed by them and the model fits reveal the above mentioned asymmetry of the secondary minimum of β Per very clearly. This asymmetry is present, though to a lesser extent, in their V light curve too. At this juncture, we have to consider whether we should expect spots at around the same position in many of these stars and if yes, why this phase interval is preferred. As Arévalo & Lázaro (1990) pointed out, absorption by a properly oriented gas stream can produce this type of effect around the phases mentioned above. Such a stream can also mimic a high bolometric albedo of the secondary in Algols, since

TABLE 8

RESIDUALS AT DIFFERENT PARTS OF THE LIGHT CURVES

	J BAND		*K* BAND	
PHASE INTERVAL	Arithmetic Mean	rms	Arithmetic Mean	rms
	$A_2 = 0.5$			
0.000–0.085.....	−0.00132	.01880	−0.00235	0.00842
0.085–0.250.....	−0.00127	.02358	+0.00108	0.00658
0.250–0.415.....	+0.01491	.02647	+0.01261	0.01924
0.415–0.500.....	+0.00290	.01928	+0.00870	0.02466
0.500–0.585.....	−0.00127	.01951	+0.00382	0.01483
0.585–0.750.....	−0.00040	.02113	−0.00527	0.01657
0.750–0.915.....	+0.00316	.02414	−0.00016	0.01679
0.915–1.000.....	+0.00159	.02094	+0.00017	0.00904
	A_2 = Free Parameter			
0.000–0.085.....	−0.00192	.00572	−0.00125	0.00719
0.085–0.250.....	+0.00275	.01494	+0.00279	0.00747
0.250–0.415.....	+0.01243	.02028	+0.00685	0.01533
0.415–0.500.....	+0.00207	.00572	+0.00654	0.01965
0.500–0.585.....	−0.00768	.01715	+0.00084	0.01604
0.585–0.750.....	−0.00817	.02117	−0.01082	0.01913
0.750–0.915.....	+0.00625	.01285	+0.00167	0.01786
0.915–1.000.....	+0.00087	.00846	+0.00120	0.00916

outside the eclipse when we move toward the primary eclipse we will start seeing more and more of the primary's surface through the gas stream. This can produce a depression of the light curve when we move toward the onset of the primary eclipse, whereas a high A_2 will cause a rise in brightness when we move toward the secondary eclipse. If we look at the region outside the light curve, these two effects can mimic the same shape except for the fact that the rise in flux caused by a high A_2 will be symmetric with respect to the secondary minimum, whereas an asymmetry can be present in the change in shape of the light curve due to a gas stream because of Coriolis deviation of the stream. Repeated observations of the complete light curves of these systems are necessary to look for the migration of these maculation phenomena. In those systems, where more than one spot is modeled on the same star, if one spot is moving and another is not, then we have to doubt the presence of the latter presumed to produce the maculation around phase 0.56–0.65, or if it is confirmed to be a spot by further observations, we have to look for processes that hold it at a particular location on the star. In this study, we have not fitted this depression in the *J*-band light curve with an additional spot on the secondary.

3.2. *Analysis of the UBV Light Curves*

The light curves published by Chambliss (1976) in the optical *U*, *B*, and *Y* bands (similar to the standard *UBV* filters) are of very good accuracy. Chambliss has analyzed the light curves by Wood's method, where the stars are

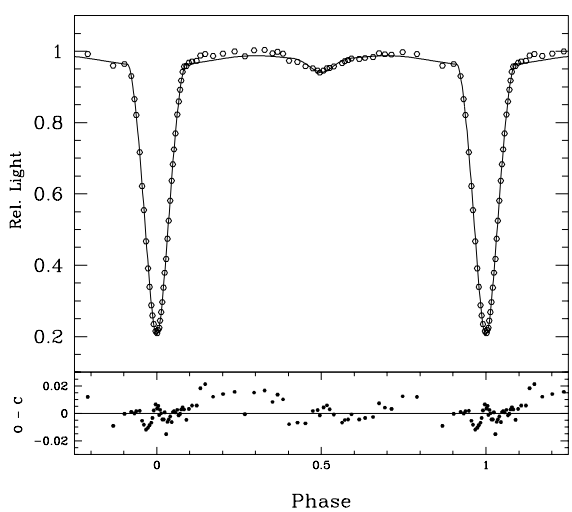

FIG. 9.—*U*-band light curve of RZ Cas and the residuals. The hexagons in the top panel show the normal points formed from the observed light curve, and the solid line shows the model fit with $A_2 = 0.5$. The bottom panel shows the deviations of the observed points from the model.

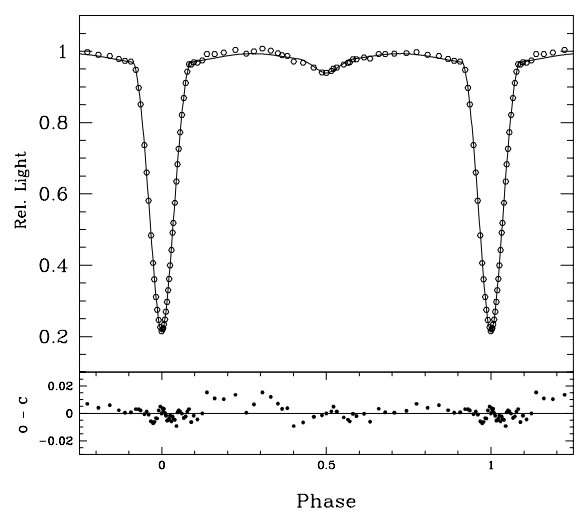

FIG. 10.—*B*-band light curve of RZ Cas and the residuals. The hexagons in the top panel show the normal points formed from the observed light curve, and the solid line shows the model fit with $A_2 = 0.5$. The bottom panel shows the deviations of the observed points from the model.

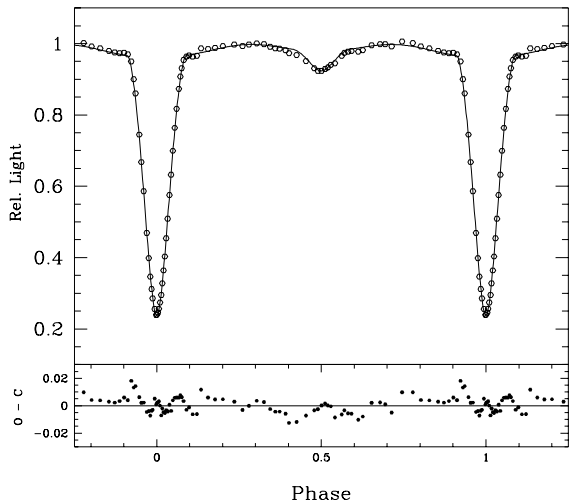

FIG. 11.—V-band light curve of RZ Cas and the residuals. The hexagons in the top panel show the normal points formed from the observed light curve, and the solid line shows the model fit with $A_2 = 0.5$. The bottom panel shows the deviations of the observed points from the model.

treated as triaxial ellipsoids, and Narusawa et al. (1994) have analyzed these light curves with the program LIGHT2 of Hill (1979). No solutions of these light curves have been obtained with Wilson's method. So we have analyzed the light curves with Wilson's program. We have used the normal points given in the Tables VI, VII, and VIII of Chambliss. The UBY light curves were analyzed separately as well as together, and the derived values of the parameters are given in Table 7. We have adopted limb darkening coefficients in the three bands as given by Narusawa et al. (1994) as fixed parameters. The values of q, T_1, and A_1 are adopted as in the case of the J and K light curves. A_2, when left as a free parameter, always stayed near its expected value 0.5 and so it is fixed to the theoretical value. Chambliss has used a low value of A_2 (0.2) in his analysis. Maxted et al. obtained high values of A_2 in the U and B bands contrary to what we find. The value of the inclination, i, derived from all the three bands match very well among themselves, but, they are larger by 1° than the value obtained by Chambliss. The parameter T_2 yields different values in the three wavelengths, with the maximum at B. T_{2V} is found to be less than T_{2U} by 140 K. This difference is only slightly more than the error limits in the value of T_2 derived by us. The value of T_2 derived by us (4507 K from the combined fit) is less than that obtained by Chambliss (1976). He obtained a gradually decreasing T_2, from 5511 K in the U band to 5006 K in the V band with an average of 5248 K in the UBV bands and a difference of 500 K in the T_2 derived from the U and the V bands. Chambliss has adopted a high value of T_1 (9700 K). Figures 9, 10, and 11 show the model light curves derived in the U, B, and V bands along with the normal points given by Chambliss (1976). As noticed by Chambliss, we can see that the residuals are not random and are distributed systematically above or below the model curve at different phases. The phases of the deviations are well correlated in all three bands. The observed secondary eclipses appear broader than the secondary eclipse of the fit that is more pronounced in the V-band light curve. There are small positive residuals around the primary minimum, which decrease to negative values at phase ~ 0.03 on both sides of the primary minimum in the U band and at phase ~ 0.02 in the V band and again increasing to positive values when the stars come out of eclipse. The presence of circumstellar gas around the primary star can be the reason for this particular distribution of the residuals around the primary minimum and the apparently broader secondary eclipse.

4. COLORS AND SPECTRAL TYPES OF INDIVIDUAL COMPONENTS

Study of photometric light curves allows us to determine the colors of individual components of a binary system. The magnitudes and colors of the individual components of RZ Cas are derived adopting the following procedure. First, the model fits were done to the J and K light curves observed by us and the UBV light curves of Chambliss (1976). Wilson's program gives the light contributions from individual components along with the total system light at each phase. These light values at phase 0.25 along with the observed magnitudes at that phase were used to calculate the magnitudes of the component stars.[3] No reddening corrections were applied as previous observers have pointed out that RZ Cas (at a distance of 73 pc) is probably unaffected by interstellar reddening (Narusawa et al. 1994).

4.1. *Primary Component*

Chambliss (1976) has classified the primary star as A2 V from his photometric analysis. Spectroscopic investigation by Duerbeck & Hanel (1979) has revealed the primary component to be an A3 V star with reasonably good accuracy. Narusawa et al. (1994) have shown the primary to be an unreddened main-sequence A3 star with solar type composition by the comparison of the IUE spectrum of RZ Cas with standard star spectra and from the Strömgren $(u - b)$, $(v - b)$, and $(b - y)$ indices. The UV colors derived by them [$(2740 - V)$, $(2365 - V)$, and $(1565 - V)$] were representative of an A4–A5 V star. But the authors have cautioned about taking these colors very seriously because of the uncertainty in the information of the phase of eclipse of RZ Cas at the time of the IUE observations. Also, the presence of a stream or hot spot can contaminate the observed UV colors.

We have derived the colors of the primary star from our photometric analysis as mentioned above. Magnitudes and colors of the system and individual components are given in Table 9. The $U-V$ color of the primary corresponds to an A3–A3.5 V star that is very close to the spectral type A3 V derived from spectroscopic studies. $B-V$, $V-J$, $V-K$ and $J-K$ colors of the primary match with the colors of an A4 V star. The intrinsic colors given by Johnson (1966) are used for comparison. Though these deviations of the spectral

[3] The magnitudes calculated will be affected by departures in the shape of the stars from spherical symmetry and the associated gravity darkening and contamination by the reflection effect. These effects will be negligible for the primary of an Algol-type system, where the distortion of the primary's surface is less and the reflected component of the light is $\sim 0.03\%$ of the intrinsic contribution of the light from the primary component. But for the secondary star, the above mentioned effects (reflected component is more than 2% of the intrinsic contribution at 0.25 phase) can cause observable contamination in the calculated colors. Also, a disk, stream or spot, not properly taken care of in the model can contaminate the derived colors.

TABLE 9

MAGNITUDES AND COLORS OF RZ CASSIOPEIAE AND ITS COMPONENTS

Photometric Band	System	Primary	Secondary
U	6.40	6.46	9.65
B	6.32	6.39	9.51
V	6.18	6.27	8.91
J	5.76	6.04	7.37
K	5.50	5.98	6.63
$U-B$	0.08	0.07	0.14
$U-V$	0.22	0.18	0.74
$B-V$	0.14	0.12	0.61
$V-J$	0.42	0.23	1.54
$V-K$	0.68	0.30	2.28

type from the spectroscopic value are minor, we have to note that it appears systematically in all bands. We would also like to point out that an A4–A5 V spectral type was derived by Narusawa et al. from UV colors. Since the errors of our photometric observations are of the order of 0.03 and 0.04 mag in the J and K bands, we cannot ascribe any physical meaning to these deviations at present. Considering the various points discussed above, we assign A3 V as the spectral and luminosity classes for the primary component.

4.2. *Secondary Component*

Chambliss (1976) has derived the spectral type of the secondary to be G5 V from his photometric study. The surface gravity and mean radius obtained by Chambliss are indicative of luminosity class III and IV, respectively. The magnitudes and colors of the secondary were derived in the present work from the photometric analysis as described in the beginning of this section. The secondary is a subgiant and no literature is available, compiling the intrinsic colors of subgiants of different spectral types. So the subgiant colors are taken as an average of the colors of main-sequence and giant stars of the same spectral type.

The $V-J$ color of 1.54 observed by us implies a K0 IV secondary, whereas the $V-K$ color, 2.28, represents a K1.5 IV star. The $J-K$ color gives us a star of K3–K3.5 IV, but this again has to be treated with caution considering the observational errors in these bands and the small value of the $J-K$ colors. The values of T_2 derived from the light curve analysis in the J and K bands are typical for a K3–K4 IV star and are lower than the temperature corresponding to our observed $V-J$ and $V-K$ colors and that derived from the analysis of the UBV light curves. Since the secondary is better observed in the J and K bands, we take the temperatures and colors in these bands to better represent this component than those derived from the optical light curves. At present we can classify the secondary as K0–K4 IV star. But the discrepancy in the optical and near-IR colors and temperatures of the secondary, and their systematic variation points to the fact that there is some factor in this system that we have not properly taken into account in the model. Further observations of this system with a view to resolving the presence of any circumstellar matter in the system could help to determine the spectral type of the components more accurately.

Figure 2 shows the observed $J-K$ color curve of RZ Cas. The $J-K$ color of the system at the primary minimum is 0.50, whereas the color of the K3.5 IV secondary component is 0.74. The observed $J-K$ color of the system at the secondary minimum is 0.17, while the color of the A3 V

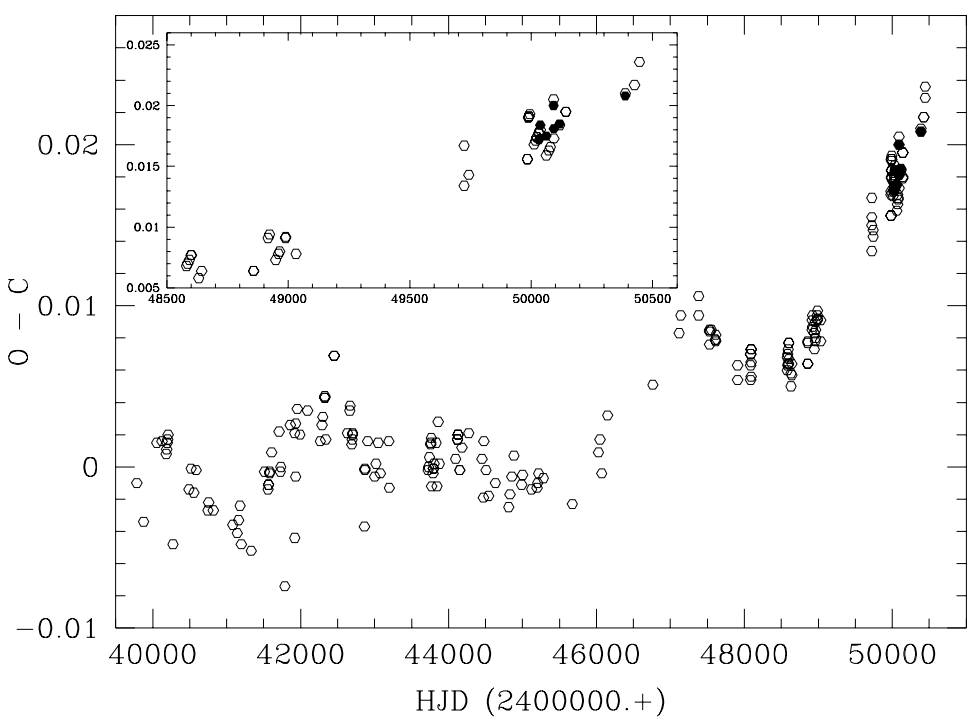

FIG. 12.—$O-C$ curve of RZ Cas showing the recent epochs of primary minima. The filled hexagons show the epochs of primary minima obtained in the present study.

primary star is 0.07. The differences in the colors are more than the observational errors. The observed colors at the minima confirm the partial nature of the eclipses.

5. PERIOD VARIATIONS

The frequent period variations of RZ Cas have inspired the interest of many people over the years (Herczeg & Frieboes-Conde 1974; Bruke & Roland 1965; Hegedus, Szatmáry, & Vinkó 1992). Kopal (1965) included RZ Cas among the list of binary systems that exhibit apsidal motion in an elliptical orbit with an eccentricity $e = 0.13$. The spectroscopic study of Horak (1952) showed a nearly circular orbit. Robinson (1965) suggested that the period might have exhibited several sudden discontinuous changes. Bruke & Roland (1965) pointed out a possible abrupt change of period around 1954. Herczeg & Frieboes-Conde (1974) interpreted the changes in $O-C$ of the times of primary minima as due to a set of period discontinuities with constant period between the jumps. They showed that some of the apparently major period changes (like the one near JD 2438300) were caused by a rapid succession of minor displacements of the epoch of primary minimum, which summed up to a measurable phase shift before the period settled down to a new value. They did not find any evidence of apsidal motion as expected in an elliptical orbit suggested by Kopal (1965). Heckathorn (1966) observed secondary minima at exactly phase 0.500, whereas Robinson (1967) observed a small shift of secondary minimum. Maxted et al. (1994) observed changes in the observed spectra associated with period changes in RZ Cas. Narusawa et al. (1994) observed that no major period changes have occurred in this system after HJD 2448581. They derived linear ephemeris for the times of minima of RZ Cas for the interval HJD 2,447,370–2,448,220 and for the observed epochs of minima after HJD 2448581 and observed that a period increase of 1.7×10^{-5} has occurred during the interval HJD 2,448,220–2,448,581.

The $O-C$ curve of RZ Cas including recent epochs of primary minima are shown in Figure 12. The values of the $O-C$ are generated with the linear epoch (Kholopov et al. 1985):

$$\text{JD Hel. Min } I = 2443200.3063 + 1.195247E_0 \text{ days} . \quad (2)$$

The epochs of seven primary minima observed in the current work are represented as filled hexagons. The recently reported epochs of minima by Narusawa et al. (1997) and Hill & Osborn (1997) are also included. The present epochs of minima show that no major period change has taken place in the system since HJD 2448581. The period derived by us is close to that of Narusawa et al. (1994). From the $O-C$ curve shown in Figure 12 it is clear that the period change was not abrupt and was continuous in the interval HJD 2448220–2448581.

6. ABSOLUTE ELEMENTS AND EVOLUTIONARY STATUS

Absolute dimensions of RZ Cas are calculated combining the separation between the components and the mass ratio from previous spectroscopic studies with the results of our photometric light curve analysis. The derived absolute dimensions are given in Table 10. The masses and radii derived in this study are higher than those derived by Chambliss (1976) but are in good agreement with those derived by Maxted et al. (1994). The mean T_2 derived in this study from the IR bands is lower than the mean T_2 of Chambliss by ~ 1000 K. Only a part of this excess (a few hundreds of K) of Chambliss can be attributed to the higher T_1 used by him. T_2 (UBV) derived from the same light curves of Chambliss in the present study is higher than the T_2 (JK) by ~ 300 K. Also, T_2 (UBV) derived by Maxted et al. is higher than T_2 (JK) by ~ 500 K. We cannot account for this difference in T_2 derived from the optical and near-IR light curves unless physical processes within the system are invoked. The significance of the physical parameters in the context of the evolutionary status of the system is described below.

TABLE 10

ABSOLUTE DIMENSIONS OF RZ CASSIOPEIAE

Parameter	Primary	Secondary
Mass ($M/M_\odot$)	2.21 ± 0.26	0.73 ± 0.07
Mean Radius ($R/R_\odot$)	1.69 ± 0.06	1.95 ± 0.06
Mean Temperature (K)	8720	4257 ± 26
Luminosity ($L/L_\odot$)	14.90 ± 1.06	1.12 ± 0.01
Mean log(g)	4.33 ± 0.02	3.72 ± 0.01
$M_{\rm bol}$	1.81 ± 0.05	4.66 ± 0.3

The H-R diagram and the position of the components of RZ Cas are shown in Figure 13*a*. The H-R diagram is adopted from the grids of Schaller et al. (1992). The solid line is the model for zero-age main-sequence (ZAMS) stars and the dotted line is for the stars at the terminal-age main sequence (TAMS) for different masses from 0.08 to 15 $M_\odot$ from Schaller et al. (1992). The broken line is adopted from Lang (1992).

We can see that the primary lies close to the ZAMS of the HR diagram and that its luminosity is normal for a main-sequence star of the same temperature. The secondary is overluminous for its spectral type, and it lies above the TAMS, implying a star evolved off the main sequence which is now a subgiant. Figure 13*b* shows the position of the components on the mass-luminosity diagram for main-sequence stars. The primary is close to main sequence though slightly underluminous for a ZAMS star of the same mass, contrary to what was found by Duerbeck & Hanel (1979). (They found a primary overluminous for its mass and interpreted it as probably evolving off the main sequence.) This behavior of the primary, being underluminous, is noticed in several Algols (Sarma, Rao, & Abhyankar 1996). The secondary is overluminous for the main sequence. Figure 13*c* shows the RZ Cas components on the main-sequence mass-temperature diagram from the models of Schaller et al. (1992). The lines and symbols are same as in Figure 13*a*. The secondary temperature is slightly lower for its mass. Figure 13*d* shows the mass-radius relation for main-sequence stars adopted from Lang (1992). The primary is seen to be slightly smaller for its mass, and the secondary is much larger than a main-sequence star. The departure of the secondary from the main sequence in the above diagrams can be interpreted as due to its evolution off the main sequence and to mass loss. We have to treat the departures of the primary with caution. The luminosity of the primary is below both the ZAMS and TAMS in the mass-luminosity diagram, whereas its temperature is lower than the ZAMS and higher than the TAMS in the mass-temperature diagram. So the primary cannot be taken as a star evolving off the main sequence. We have to treat these

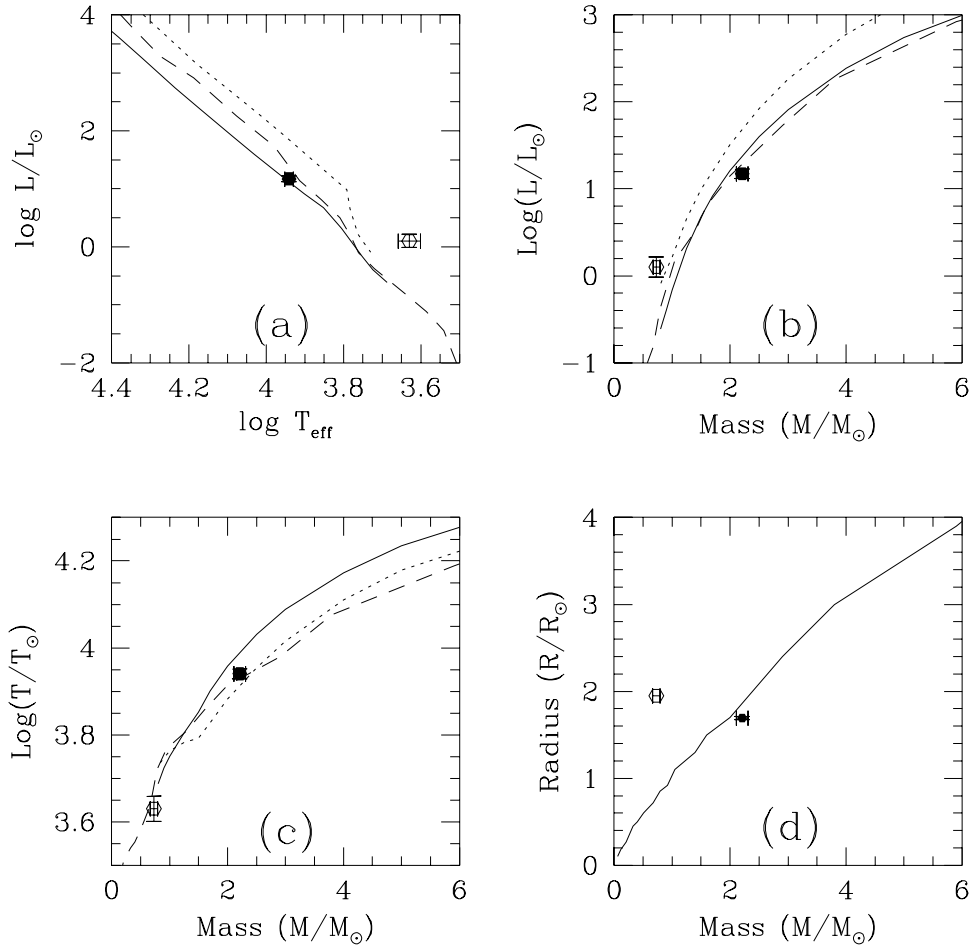

FIG. 13.—(*a*) HR diagram and the position of the components of RZ Cas. The filled hexagons represents the primary star, and the open hexagons represent the secondary star. (*b*) mass-luminosity diagram; (*c*) mass-temperature diagram; and (*d*) mass-radius diagram for main-sequence stars.

deviations from the perspective of the effects of mass transfer to a star, which has already started nuclear burning at a much lower mass.

7. CONCLUSIONS

The secondary temperature derived from the infrared bands is less than that derived from the optical bands by ~ 300 K even after adopting the same size for the primary star. Also, the derived value of the bolometric albedo of the secondary surface is higher in the IR bands (>0.7), whereas in the optical bands it is near the theoretical value for a convective atmosphere (0.5) as expected for a subgiant star of its mass. This is indicative of the deficiency of a bolometric treatment of the reflection effect in light curve modeling. Local absorption at one wavelength and reemission at a different wavelength could be a possible reason for the departures of the albedo from its theoretical value. Another possible explanation is the presence of a cool dark spot on the back side of the secondary star. When the J and K light curves were fitted with a spot on the secondary, the bolometric albedo reduced to its expected theoretical value of 0.5 and T_2 increased. A gas stream from the lobe-filling secondary to the primary star can also produce the effects mentioned above.

Secondary eclipse is asymmetric, both in the J and K bands, especially near the end of the eclipse where it shows a depression and large scatter, the effect being more prominent in the J-band light curve. This is probably due to the presence of gas streams. This type of phenomenon is seen in the IR light curves of many short-period RS CVn systems. This was also noticed before in the optical and near-infrared light curves of β Per.

Though some observers have seen a flat bottom of the primary minimum lasting for up to 21 minutes, none of the minima observed in the present study showed a flat bottom. The observed eclipse depths and colors at the minima in the IR bands also rule out any probability of a total eclipse. We can now confidently state that RZ Cas is a partially eclipsing system. The observed flat bottom that appears randomly can be a manifestation of the presence of variable amounts of circumstellar matter. A new ephemeris for the primary minima is derived from our observed epochs of the primary minima. The present values of the $O-C$ of the primary minima show that the system has not undergone any major period change during the last 5 years. The secondary minima appear at 0.5 phase, and the observed primary and secondary eclipses were of equal width, implying a circular orbit.

We thank U. S. Kamath and Anandmayee Tej of the Astronomy Division of the Physical Research Laboratory

for their help in the data collection and Tibor Hegedus of the Baja Observatory for sending us the data on the times of minima of RZ Cas, compiled by late D. Lichtenknecker. We also thank the referee for many valuable suggestions. This work is funded by the Department of Space, Government of India.

APPENDIX

This appendix contains the *J*-band (Table A1) and *K*-band (Table A2) observations of RZ Cas.

TABLE A1

J-Band Light Curve of RZ Cassiopeiae

HJD	Phase	Δm	HJD	Phase	Δm	HJD	Phase	Δm
50,031.38444.....	0.1842	0.108	50,033.30540.....	0.7913	0.071	50,035.31632.....	0.4737	0.216
50,031.38980.....	0.1887	0.107	50,033.31007.....	0.7952	0.087	50,035.31740.....	0.4746	0.219
50,031.39144.....	0.1900	0.087	50,033.31113.....	0.7961	0.069	50,035.32248.....	0.4789	0.222
50,031.39613.....	0.1940	0.064	50,033.31517.....	0.7995	0.023	50,035.32818.....	0.4837	0.258
50,031.41166.....	0.2070	0.092	50,033.31620.....	0.8004	0.039	50,035.32932.....	0.4846	0.278

Notes.—HJD = HJD + 2,400,000. Table A1 is presented in its entirety in the electronic edition of the Astronomical Journal. A portion is shown here for guidance regarding its form and content.

TABLE A2

K-Band Light Curve of RZ Cassiopeiae

HJD	Phase	Δm	HJD	Phase	Δm	HJD	Phase	Δm
49,997.27583.....	0.6476	−0.153	49,997.42292.....	0.7707	−0.072	50,000.39265.....	0.2552	−0.117
49,997.27616.....	0.6479	−0.137	49,997.43021.....	0.7768	−0.146	50,000.39728.....	0.2591	−0.133
49,997.27737.....	0.6489	−0.158	49,997.43158.....	0.7779	−0.130	50,000.39932.....	0.2608	−0.157
49,997.27774.....	0.6492	−0.136	49,997.43271.....	0.7788	−0.131	50,000.40476.....	0.2654	−0.098
49,997.28606.....	0.6562	−0.122	49,997.44008.....	0.7850	−0.105	50,000.40698.....	0.2672	−0.156

Notes.—HJD = HJD + 2,400,000. Table A2 is presented in its entirety in the electronic edition of the Astronomical Journal. A portion is shown here for guidance regarding its form and content.

REFERENCES

Al Naimiy, H. M. 1978, Ap&SS, 53, 181
Arévalo, M. J., & Lázaro, C. 1990, AJ, 99, 983
Argenbright, D. V., Osborn, W., & Hall, D. S. 1988, Inf. Bull Variable Stars 3224
Ashok, N. M., Chandrasekhar, T., Sam Ragland, & Bhatt, H. C. 1994, Exp. Astron., 4, 177
Bruke, E. W., & Roland, W. W. 1965, AJ, 71, 38
Budding, E., & Zeilik, M. 1987, ApJ, 319, 827
Carbon, D., & Gingerich, O. 1969, in Theory and Observation of Stellar Atmospheres, ed. O. Gingerich (Cambridge: MIT), 377
Chambliss, C. R. 1976, PASP, 88, 22
Chen, K. Y., & Reuning, G. 1966, AJ, 71, 283
Drake, S. A., Simon, T., & Linsky, J. L. 1986, AJ, 91, 1229
Duerbeck, H. W., & Hanel, A. 1979, A & AS, 38, 155
Elias, J. H., Frogel, J. A., Matthews, K., Neugebauer, G. 1982, AJ, 87, 1029
Hall, D. S. 1989, Space Sci. Rev., 50, 219
Heckathorn, H. M. 1966, Publ. Godsell Obs. 15
Hegedus, T. 1989, Inf. Bull. Variable Stars 3381
Hegedus, T., Szatmáry, K., & Vinkó, J. 1992, Ap&SS, 187, 57
Herczeg, T., & Frieboes-Conde, H. 1974, A&A, 30, 259
Hill, G. 1979, Publ. Dom. Astrophys. Obs. Victoria, 15, 297
Hill, J., & Osborn, W. 1997, Inf. Bull. Variable Stars 4502
Horak, H. G. 1952, ApJ, 115, 61
Huffer, C. M. 1955, ApJ, 121, 677
Huffer, C. M., & Kopal, Z. 1951, ApJ, 114, 297
Johnson, H. L. 1966, ARA&A, 4, 193
Kholopov, P. N., et al. 1985, The General Catalogue of Variable Stars, Vol. 1 (Moscow: Nauka)
Kopal, Z. 1965, Adv. Astron. Astrophys., 3, 105
Kwee, K. K., & van Woerden, H. 1956, Bull. Astron. Inst. Netherlands, 12, 327
Lang, K. R. 1992, Astrophysical Data: Planets and Stars (New York: Springer)
Lazaro, C., Martinez-Pais, I. G., Arevalo, M. J., & Antonopoulou, E. 1997, AJ, 113, 1122
Lucy, L. B. 1967, Z. Astrophys., 65, 89
Maxted, P. F. L., Hill, G., & Hilditch, R. W. 1994, A&A, 282, 821
McCluskey, G. E., Jr. 1993, in The Realm of Interacting Binary Stars, ed. J. Sahade, G. E. McCluskey, Jr., & Y. Kondo (Dordrecht: Kluwer), 39
McCluskey, G. E., Jr., & Kondo, Y. 1984, PASP, 96, 817
Narusawa, S. Y., Arai, K., Nagai, K., Ohmori, S., Fujii, M., & Yasuda, T. 1997, Inf. Bull. Variable Stars 4502
Narusawa, S. Y., Nakamura, Y., & Yamasaki, A. 1994, AJ, 105, 1141
Neugebauer, G., & Lighton, R. B. 1969, Two Micron Sky Survey: A Preliminary Catalog (NASA SP-3047)
Olson, E. C. 1982, ApJ, 259, 702
Riazi, N., Bagheri, M. R., & Faghihi, F. 1994, Ap&SS, 211, 293
Richards, M. T. 1990, ApJ, 350, 372
Richards, M. T., Mochnacki, S. W., & Bolton, C. T. 1988, AJ, 96, 326
Robinson, L. J. 1965, Inf. Bull. Variable Stars 112
———. 1967, Inf. Bull. Variable Stars 180
Rucinski, S. M. 1969, Acta Astron., 19, 245
Sam Ragland. 1996, Ph. D. thesis, Indore Univ.
Sarma, M. B. K., Rao, P. V., & Abhyankar, K. D. 1996, ApJ, 458, 371
Schaller, G., Schaerer, D., Meynet, G., & Maeder, A. 1992, A & AS, 96, 269
Schmitt, J. H. M. M., Collura, A., Sciortino, S., Vaiana, G. S., Harnden, F. R., Jr., & Rosner, R. 1990, ApJ, 365, 704
Scott, J. K. 1988, AJ, 96, 337
Singh, K. P., Drake, S. A., & White, N. E. 1995, ApJ, 445, 840
Szafraniec, R. 1960, Acta Astron., 10, 99
Umana, G., Catalano, S., & Rodono, M. 1991, A&A, 249, 217
Umana, G., Trigilio, C., Hjellming, R. M., Catalano, S., & Rodono, M. 1993, A&A, 267, 126
Van Hamme, W. 1993, AJ, 106, 1096
Van Hamme, W., & Wilson, R. E. 1986, AJ, 92, 1168
———. 1990, AJ, 100, 1981
———. 1993, MNRAS, 262, 220
Von Zeipel, H. 1924, MNRAS, 84, 665, 684, 702
Wilson, R. E. 1979, ApJ, 234, 1054
———. 1990, ApJ, 356, 613
———. 1993, in ASP Conf. Ser. 38, New Frontiers in Binary Star Research, ed. K. C. Leung & I. S. Nha (San Francisco: ASP), 91
Wilson, R. E., De Luccia, M., Johnston, K., & Mango, S. A. 1972, ApJ, 177, 191
Wilson, R. E., & Devinney, E. J. 1971, ApJ, 166, 605